Electronic Supplementary Material (ESI) for Journal of Materials Chemistry A.

Supporting Information for "Enhanced Urea Oxidation Catalysis through Ni Single-Atom Doping on Cu_2O Surfaces: A Computational Study"

Xiaoqing Li,[a] Haiping Lin,[b] Wenjing Huang,[a,*] Shiyun Xiong,[a,*] Shaoming Huang[a,*]

[a] School of Materials and Energy, Guangdong University of Technology, Guangzhou 510006, Guangdong, China. E-mail: wjhuang42@gdut.edu.cn; syxiong@gdut.edu.cn; smhuang@gdut.edu.cn.

[b] School of Physics and Information Technology, Shaanxi Normal University, Xian 710119, Shaanxi, China.

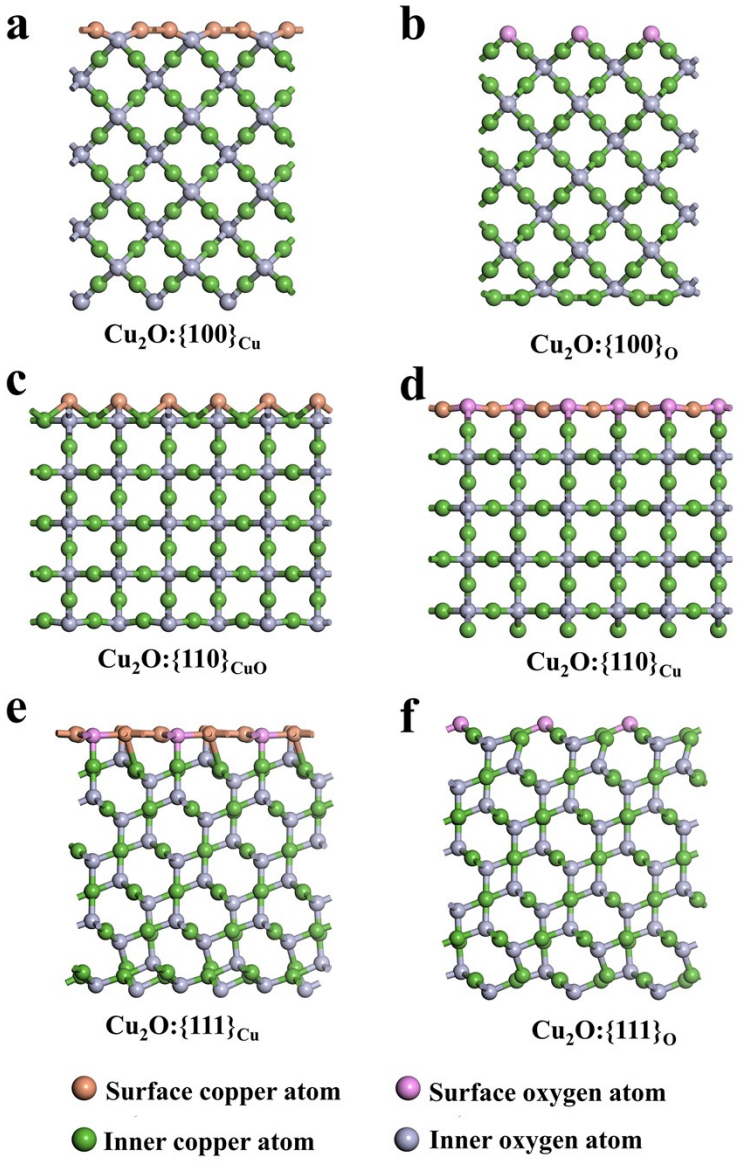

Fig. S1 Side view of the six low-index surfaces of Cu_2O after relaxation. In the Cu_2O:$\{111\}_{Cu}$ structure, the surface Cu atoms are relaxed to the same atomic plane as the subsurface O atoms.

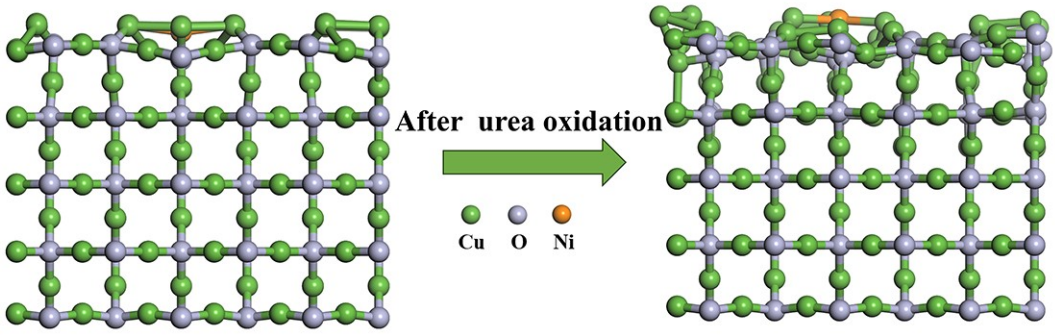

Fig. S2 Surface reconstruction of Ni-Cu_2O:$\{110\}_{Cu}$ during urea adsorption process. Left: before urea adsorption; Right: after urea adsorption.

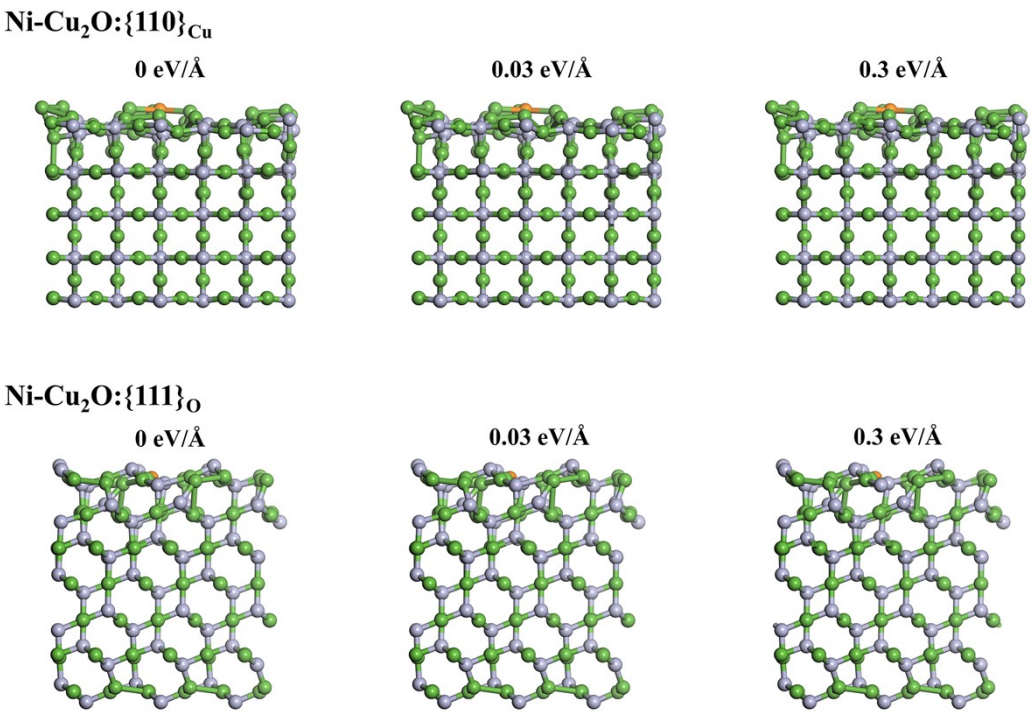

Fig. S3 The optimized structures for Ni-Cu_2O:$\{110\}_{Cu}$ and Ni-Cu_2O:$\{111\}_{O}$ under different electric fields.

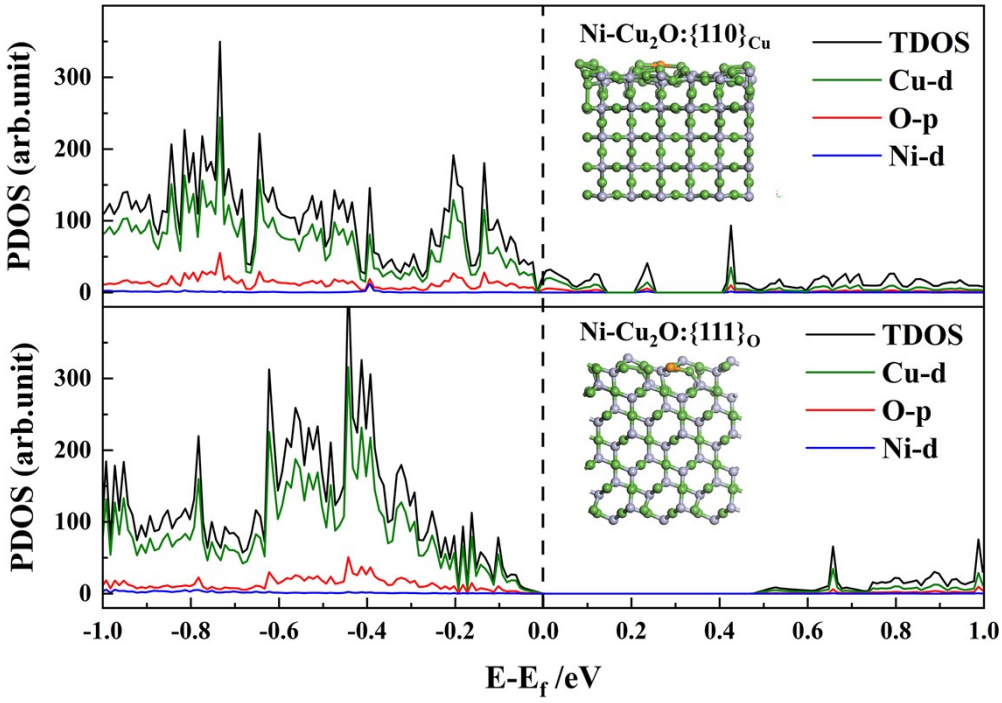

Fig. S4 TDOS and PDOS of Cu-d, Ni-d, and O-p orbitals in Ni-Cu_2O:{110}$_{Cu}$ (top) and Ni-Cu_2O:{111}$_O$ (bottom). Orange, green, and silver colors denote Ni, Cu, and O atoms, respectively.

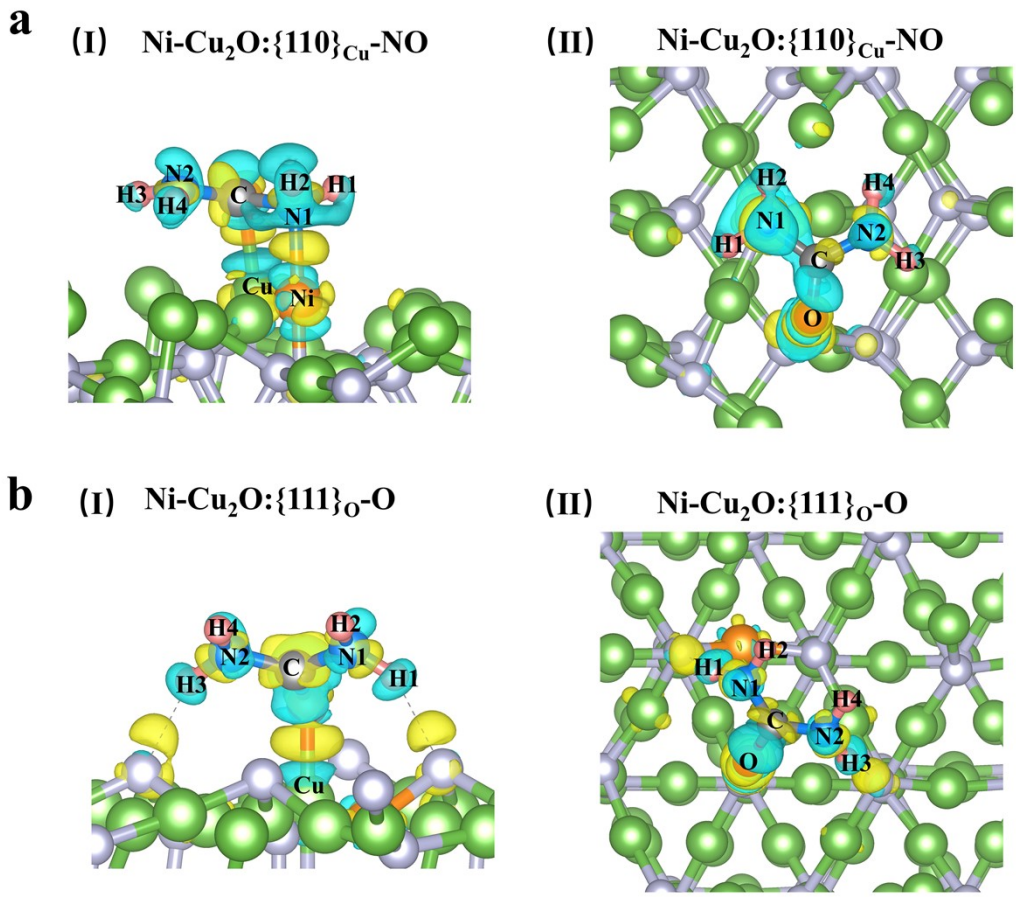

Fig. S5 Differential charge density maps for Ni-Cu_2O:{110}$_{Cu}$-NO (a) and Ni-Cu_2O:{111}$_O$-O (b). The side and top views are illustrated in (I) and (II) of the corresponding subfigure. In all plots, the isosurface is set to 0.003 eÅ^{-3}.

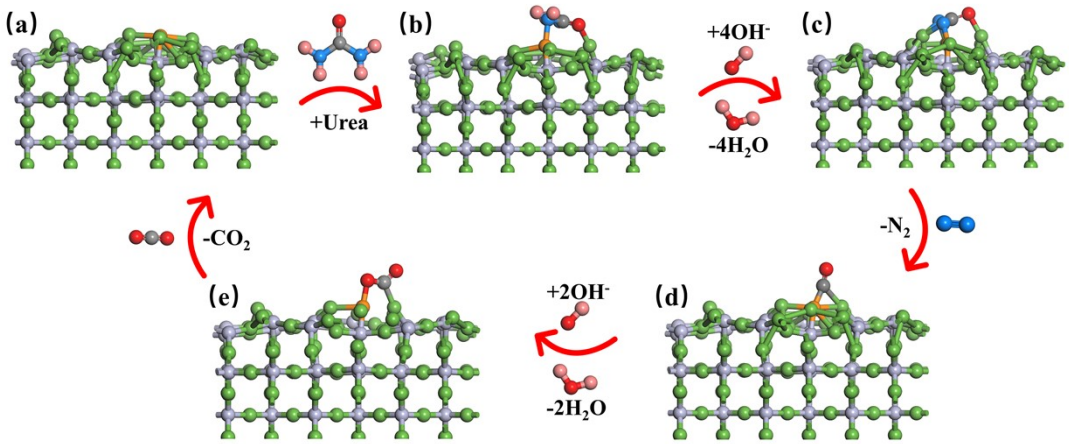

Fig. S6 Schematic diagram of the reaction path flow for the oxidation of urea to N_2 and CO_2.

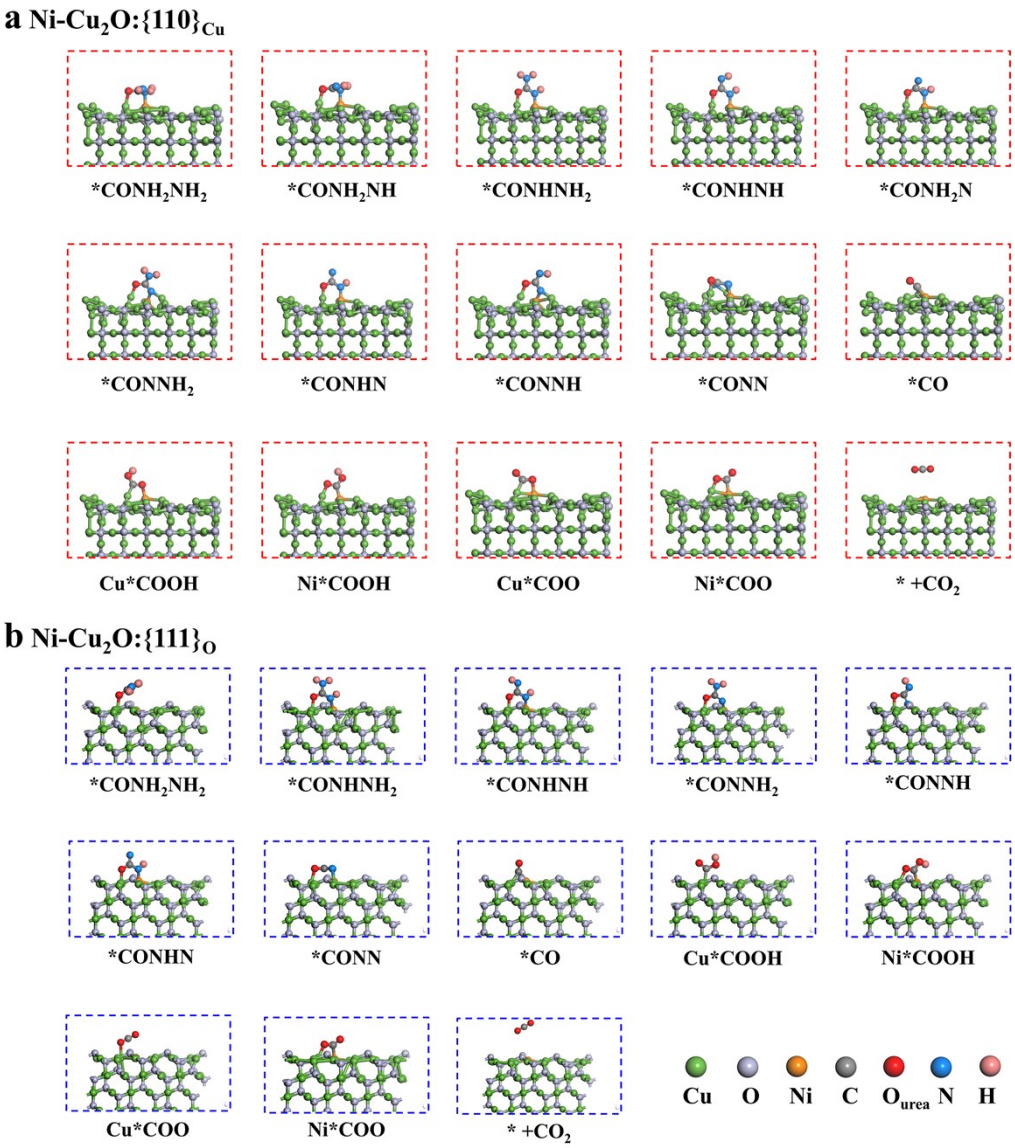

Fig. S7 Optimized atomic structures of various intermediates during UOR reaction for(a) Ni-Cu_2O:{110}$_{Cu}$-NO and (b) Ni-Cu_2O:{111}$_O$-O.

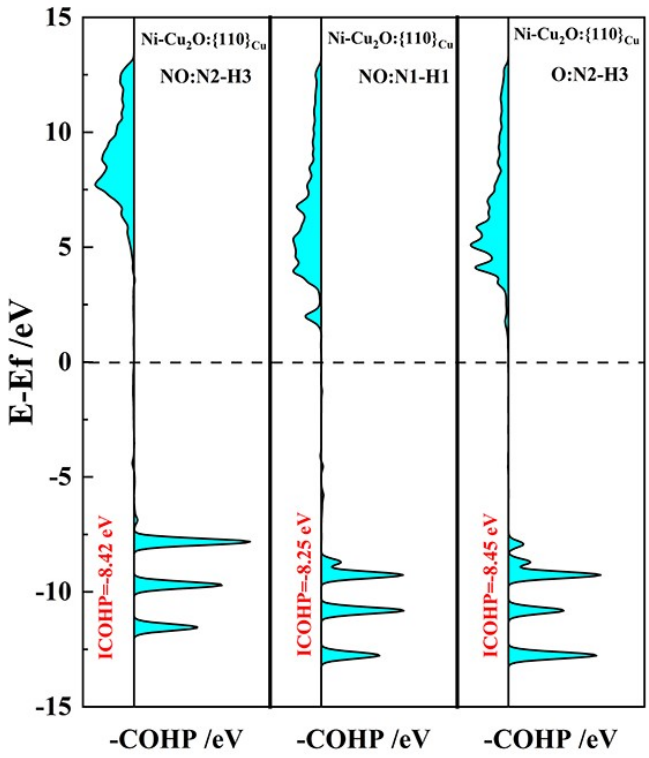

Fig. S8 Variation of -COHP with energy for the N-H bonds in Ni-Cu_2O:{110}$_{Cu}$-NO and Ni-Cu_2O:{111}$_O$-O.

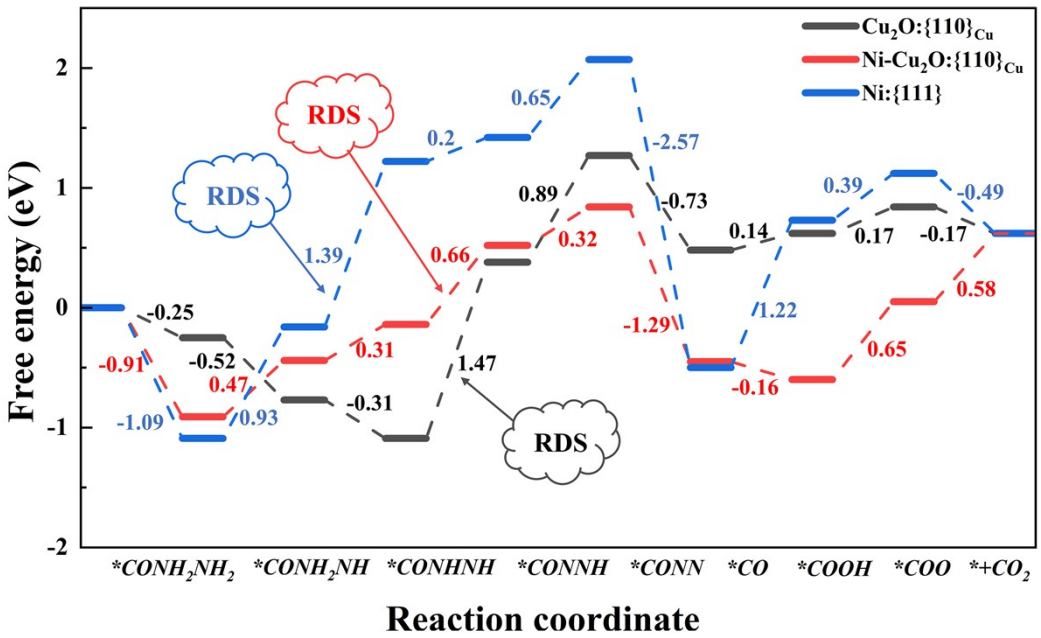

Fig. S9 Gibbs free energies of each intermediate during UOR on Ni:{111}, Cu_2O:{110}$_{Cu}$, and Ni-Cu_2O:{110}$_{Cu}$.

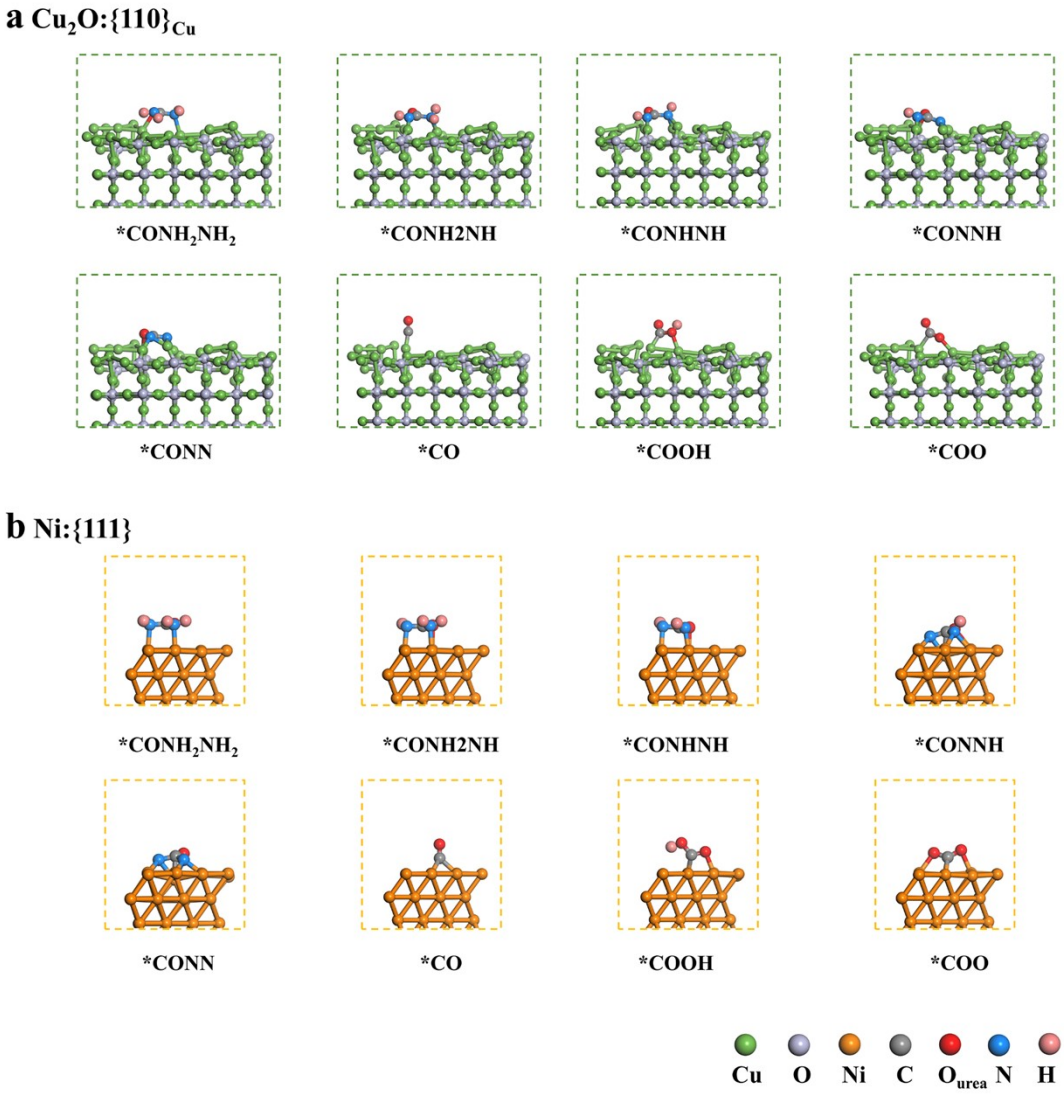

Fig. S10 Optimized atomic structures of various intermediates during UOR reaction for (a) Cu_2O:{110}$_{Cu}$ and (b) Ni:{111}.

Table S1. Gibbs free energies, zero-point energies, and entropies of the reaction intermediates in Ni-Cu_2O:{111}$_O$ and Ni-Cu_2O:{110}$_{Cu}$ catalysts.

Species	ZPE (eV) Ni-Cu_2O:{110}$_{Cu}$	TS (eV) Ni-Cu_2O:{110}$_{Cu}$	ZPE (eV) Ni-Cu_2O:{111}$_O$	TS (eV) Ni-Cu_2O:{111}$_O$
***$CONH_2NH_2$**	1.75	0.28	1.74	0.31
***$CONH_2NH$**	1.42	0.25	\	\
***$CONHNH_2$**	1.43	0.25	1.14	0.26
***CONHNH**	1.06	0.25	1.06	0.25
***$CONH_2N$**	1.06	0.26	\	\
***$CONNH_2$**	1.10	0.23	1.09	0.23
***CONHN**	0.74	0.23	0.72	0.24
***CONNH**	0.75	0.21	0.72	0.24
***CONN**	0.46	0.13	0.44	0.17
***CO**	0.20	0.10	0.2	0.15
Cu*COOH	0.64	0.17	0.61	0.22
Ni*COOH	0.64	0.18	0.56	0.18
Cu*COO	0.31	0.18	0.32	0.19
Ni*COO	0.31	0.16	0.32	0.19

Table S2. The d-band center ε_d of the active sites before and after urea molecules adsorption. For urea molecules adsorbed by dual active sites, we adopt the method in Ref [1].

Catalyst	ε_d (eV) before adsorption	ε_d (eV) after adsorption
Ni-Cu_2O:{110}$_{Cu}$	-1.47	-1.77
Ni-Cu_2O:{111}$_O$	-1.21	-1.02

Table S3. Comparison of urea adsorption energy, overpotential, and CO_2 desorption energy in various UOR electrocatalysts reported in literatures. The UOR mechanisms in literatures include both conventional adsorption mechanisms and lattice oxygen mechanisms (LOM). The ΔG_{max} of dehydrogenation epresents the maximum dehydrogenation reaction energy.

Catalyst	ΔG_{max} of dehydrogenation (eV)	CO_2 desorption energy (eV)	Overpotential (V)	Ref.
Ni-Cu_2O:{110}$_{Cu}$	**0.66**	**0.58**	**0.29**	**This work**
NiOOH	1.44	0.9	1.07	[2]
NiOO (LOM)	0.96	0.4	0.59	[2]
LNO-2	0.69	1.05	0.68	[3]
LNO-2 (LOM)	0.69	0.11	0.32	[3]
CoNi@CN-CoNiMoO	1.15	-0.32	0.78	[4]
O_{vac}-V-Ni$(OH)_2$	2.35	0.67	1.98	[5]
Ac-CoOCl-V	2.05	-0.74	1.68	[6]
Ru-Co DAS/NiO	1.63	0.56	1.26	[7]

Table S4. Calculated d-band centers for *COO intermediate. For Ni-Cu_2O:{111}$_O$-Cu*COO, CO_2 is adsorbed solely by a Cu atom, while for other structures, CO_2 is adsorbed by multiple active sites.

Species	ε_d (eV)
Ni-Cu_2O:{110}$_{Cu}$-Ni*COO	-1.41
Ni-Cu_2O:{110}$_{Cu}$-Cu*COO	-1.82
Ni-Cu_2O:{111}$_O$-Ni *COO	-1.53
Ni-Cu_2O:{111}$_O$-Cu*COO	-1.67

Table S5. Gibbs free energies, zero-point energies, and entropies of the reaction intermediates for Ni:{111} and Cu_2O:{110}$_{Cu}$ catalysts.

Species	ZPE (eV) Ni:{111}	TS (eV) Ni:{111}	ZPE (eV) Cu_2O:{110}$_{Cu}$	TS (eV) Cu_2O:{110}$_{Cu}$
***$CONH_2NH_2$**	1.71	0.2	1.73	0.30
***$CONH_2NH$**	1.40	0.25	1.45	0.21
***CONHNH**	1.07	0.20	1.16	0.25
***CONNH**	0.72	0.17	0.78	0.16
***CONN**	0.43	0.14	0.46	0.14
***CO**	0.19	0.14	0.19	0.18
***COOH**	0.59	0.16	0.59	0.16
***COO**	0.28	0.18	0.29	0.23

References:

1 S. Ponath, M. Menger, L. Grothues, M. Weber, D. Lentz, C. Strohmann and M. Christmann, *Angew. Chem. Int. Ed.*, 2023, **62**, e202216920.

2 L. Zhang, L. Wang, H. Lin, Y. Liu, J. Ye, Y. Wen, A. Chen, L. Wang, F. Ni, Z. Zhou, S. Sun, Y. Li, B. Zhang and H. Peng, *Angew. Chem. Int. Ed.*, 2019, **58**, 16820-16825.

3 W.-K. Han, J.-X. Wei, K. Xiao, T. Ouyang, X. Peng, S. Zhao and Z.-Q. Liu, *Angew. Chem. Int. Ed.*, 2022, **61**, e202206050.

4 G. Qian, J. Chen, W. Jiang, T. Yu, K. Tan and S. Yin, *Carbon Energy*, 2023, **5**, e368.

5 H. Qin, Y. Ye, J. Li, W. Jia, S. Zheng, X. Cao, G. Lin and L. Jiao, *Adv. Funct. Mater.*, 2023, **33**, 2209698.

6 B. Zhang, C. Pan, H. Liu, X. Wu, H. Jiang, L. Yang, Z. Qi, G. Li, L. Shan, Y. Lin, L. Song and Y. Jiang, *Chem. Eng. J.*, 2022, **439**, 135768.

7 X. Zheng, J. Yang, P. Li, Z. Jiang, P. Zhu, Q. Wang, J. Wu, E. Zhang, W. Sun, S. Dou, D. Wang and Y. Li, *Angew. Chem. Int. Ed.*, 2023, **62**, e202217449.